

New dynamical observer for a batch crystallization process based on solute concentration

Lucas Brivadis¹, Vincent Andrieu¹, Élodie Chabanon¹, Émilie Gagnière¹, Noureddine Lebaz¹,
and Ulysse Serres¹

¹Univ Lyon, Université Claude Bernard Lyon 1, CNRS, LAGEPP UMR 5007, 43 boulevard du
11 novembre 1918, F-69100, Villeurbanne, France

June 15, 2020

Abstract

In this paper a new observer is introduced to estimate the Crystal Size Distribution (CSD) only from the measurements of the solute concentration, temperature and a model of the growth rate. No model of the nucleation rate is needed. This approach is based on the use of a Kazantzis-Kravaris/Luenberger observer which exponentially estimates functionals of the CSD. Then, the full state is estimated by means of a Tikhonov regularization procedure. Numerical simulations are provided. Our approach relies on an infinite-dimensional observer, contrarily to the usual moment based observers.

Keywords: Observers, Crystallization, Crystal Size Distribution, Tikhonov regularization, Solute concentration

1 Introduction

Crystallization is one of the oldest and major processes used in industry (chemical, pharmaceutical, food, etc.) to produce, purify or separate solid compounds or products [4]. This unit operation aims to produce solid crystals with well defined specifications including (among others) the Crystal Size Distribution (CSD) which is of critical importance. At the industrial scale, the CSD is neither well controlled nor monitored during the crystallization process and a grinding step is usually performed before delivering the final product. Hence, a key point is the real-time control and the “*online*” monitoring of the CSD during the crystallization operation in order to avoid the grinding step. Unfortunately, the CSD is nowadays not directly measurable in real-time by existing sensors. Nevertheless, the Process Analytical Technologies (PATs) allow us to get access to real time information such as the solute concentration based on the Attenuated Total Reflectance Fourier Transform InfraRed spectroscopy (ATR-FTIR) and the Chord Length Distribution based on the Focused Beam Reflectance Measurement (FBRM[®]). FBRM[®] is commonly employed in pharmaceutical industries to detect online some process deviations. Note however that its use for online estimation of the CSD remains challenging [24, 27].

Obtaining an online CSD estimation from the solute concentration, temperature and a growth rate model only is an interesting problem which is the purpose of the present paper. To obtain online state estimation for dynamical systems from measured outputs, control engineers usually employ asymptotic state observers. Designing state observer for complex dynamical systems is an active research area. Some studies are devoted to nonlinear dynamics (see [2] and references therein). Others consider infinite dimensional systems (see for instance [28]).

Designing observers for a batch crystallization process has been addressed in recent years by several researchers (see for instance [17, 18, 19, 21, 25, 29, 30]). These studies are based on spatial discretization of the PDE (see [25] or [30]) or more frequently on moments analysis (see survey [18]). However, the moment based approaches suffer from several drawbacks: (i) the numerical moment values exhibit a very large difference in their order of magnitude [10]. Consequently, a small numerical/experimental error has a significant impact on the moments estimation. The error will then be propagated during the computation of the moment transport equations [7]; (ii) the recovering of the CSD from a finite number of its moments is still an open area of research in mathematics and highly dependant of the moments quality [13, 23]. Furthermore, the moment based observers depend on the knowledge of the nucleation rate which may be tricky to model. All these reasons may explain the difficulty to develop an efficient algorithm following this route.

In this paper, another approach is adopted to describe the CSD without using its moments. Moreover, a key point of the proposed approach is that no information is needed on the nucleation rate.

In the first part of the paper, we recall the Kazantzis-Kravaris/Luenberger methodology for observer design which has been introduced in its original form in [14] for linear systems and adapted for nonlinear dynamics in [1] and [11]. Section 3 is devoted to the modeling of the batch crystallization process. Finally some simulation results are presented in Section 4 which highlight the practical interest of the suggested methodology.

2 Kazantzis-Kravaris/Luenberger observer methodology

In control engineering, the algorithm which is employed to reconstruct online missing data on a partially measured dynamical process is named an observer. Observer design for nonlinear dynamical systems is a very active research area and has been the subject of numerous studies in the past 40 years (see [2] for a recent survey on this topic). One very efficient way to design observers for finite-dimensional linear as well as nonlinear dynamical systems is the Kazantzis-Kravaris/Luenberger (KKL) observer methodology. It is an approach which follows Luenberger original idea in [14] where asymptotic observers for linear systems were introduced for the first time. The approach of [14] is somehow different from the way *Luenberger observers* are introduced nowadays (which follows Luenberger second paper on observers [15]). It has been recently employed by Kazantzis and Kravaris in [11] to design local observers for finite-dimensional nonlinear dynamics based on Luenberger original idea in a local version. We hope it may also be fruitful in the context of distributed parameter systems. In this section we adapt to the context of linear abstract Cauchy problem the KKL observer methodology which is a two-steps design procedure. In the first step we consider the problem of estimating a function of the state. The reconstruction of the overall state of the system is obtained in the second step by inverting this function.

2.1 Step 1: reconstruction of a function of the state

As shown in [1] and [3], it is always possible to exponentially estimate a function of the state, even for nonlinear finite-dimensional systems, that will carry enough information about the state to estimate it in Step 2. In order to

do so, it is sufficient to introduce an auxiliary dynamical system fed by the measured output such that its solutions provide an estimation of this function of the state.

Let \mathbb{R} (resp. \mathbb{R}_+ , \mathbb{R}_- and \mathbb{R}^*) denotes the set of real numbers (resp. non-negative, non-positive and non-zero real numbers). Let \mathcal{X} be a Hilbert space. We denote $\mathcal{L}(\mathcal{X})$ the set of all endomorphisms of \mathcal{X} and $\mathcal{L}(\mathcal{X}, \mathbb{R})$ the space of linear forms from \mathcal{X} to \mathbb{R} . Consider the abstract Cauchy problem on \mathcal{X}

$$\dot{\psi} = \mathcal{F}\psi, \quad \psi(0) = \psi_0, \quad (1)$$

where $\mathcal{F} : D(\mathcal{F}) \subset \mathcal{X} \rightarrow \mathcal{X}$ is a linear operator which is the generator of a strongly continuous semi-group denoted $(T_t)_{t \in \mathbb{R}_+}$ in $\mathcal{L}(\mathcal{X})$ and $\psi_0 \in D(\mathcal{F})$. Let $\rho(\mathcal{F}) = \{\lambda \in \mathbb{C} \mid (\mathcal{F} - \lambda I)^{-1} \in \mathcal{L}(\mathcal{X})\}$ denote the resolvent set of \mathcal{F} . Moreover, consider a bounded output operator

$$y = \mathcal{H}\psi, \quad (2)$$

where $\mathcal{H} \in \mathcal{L}(\mathcal{X}, \mathbb{R})$ is bounded. Following the KKL methodology, we obtain the following proposition.

Proposition 2.1. *For all λ in $\rho(\mathcal{F}) \cap \mathbb{R}^*$, let \mathcal{T}_λ in $\mathcal{L}(\mathcal{X}, \mathbb{R})$ be the operator defined as*

$$\mathcal{T}_\lambda : \mathcal{X} \ni \psi \mapsto \mathcal{H}(\mathcal{F} - \lambda I)^{-1}\psi \in \mathbb{R}.$$

Then, the dynamical system

$$\dot{z}_\lambda = \lambda z_\lambda + y, \quad (3)$$

is an exponential observer for $\mathcal{T}_\lambda\psi$. More precisely, for all (ψ_0, z_0) in $D(\mathcal{F}) \times \mathbb{R}$, it yields for all $t \geq 0$

$$\mathcal{T}_\lambda(T_t\psi_0) - z_\lambda(t) = \exp(\lambda t) (\mathcal{T}_\lambda(\psi_0) - z_0). \quad (4)$$

where $z_\lambda : \mathbb{R}_+ \rightarrow \mathbb{R}$ is the solution of system (3) when y is given by (2) and initiated from z_0 .

Proof. Let ψ_0 be in $D(\mathcal{F})$. Equations (1)–(3) yield

$$\begin{aligned} \frac{d}{dt}(\mathcal{T}_\lambda(T_t\psi_0) - z_\lambda(t)) &= \mathcal{T}_\lambda(\mathcal{F}T_t\psi_0) - \lambda z_\lambda(t) - \mathcal{H}T_t\psi_0 \\ &= \mathcal{T}_\lambda(\mathcal{F} - \lambda I)T_t\psi_0 + \lambda(\mathcal{T}_\lambda(T_t\psi_0) - z_\lambda(t)) - \mathcal{H}T_t\psi_0 \\ &= \lambda(\mathcal{T}_\lambda(T_t\psi_0) - z_\lambda(t)), \end{aligned}$$

where the last equality follows since $\mathcal{T}_\lambda(\mathcal{F} - \lambda I) = \mathcal{H}$. Hence, (4) follows by integrating in time the former equation.

Keeping in mind that λ is negative in Proposition 2.1, (4) implies

$$\lim_{t \rightarrow +\infty} |\mathcal{T}_\lambda(T_t\psi_0) - z_\lambda(t)| = 0. \quad (5)$$

This ends the proof. □

Remark 1. *The operator \mathcal{T}_λ is solution to the Sylvester equation :*

$$\mathcal{F}\mathcal{T}_\lambda = \lambda\mathcal{T}_\lambda + \mathcal{H}. \quad (6)$$

We recognize here the algebraic equation which was already given in Luenberger seminal paper [14] and which becomes a nonlinear partial differential equation in [1].

2.2 Step 2: reconstruction of the entire state of the system

According to step 1, we can easily estimate $\mathcal{T}_\lambda \psi$ for all λ in $\rho(\mathcal{F}) \cap \mathbb{R}_+^*$ via the observer system (3). The idea of the KKL observer methodology is to consider the mapping $\mathcal{T} : \mathcal{X} \mapsto \mathbb{R}^p$ given by $\psi \mapsto (\mathcal{T}_{\lambda_1} \psi, \dots, \mathcal{T}_{\lambda_p} \psi)$ which will be exponentially estimated along the trajectory of (1) via a bench of observers of the form (3). To solve the estimation problem, the question is to solve the inverse problem

$$\mathcal{T} \hat{\psi} = z \tag{7}$$

with the unknown $\hat{\psi}$ in \mathcal{X} . Let $\text{Im}\mathcal{T} = \{\mathcal{T}x \mid x \in \mathcal{X}\}$ be the image of \mathcal{T} . Then (7) admits a solution only if z is in $\text{Im}\mathcal{T}$. The former condition is in general too restrictive due to the fact that z is only an estimation of $\mathcal{T}\psi$ and consequently may not be in $\text{Im}\mathcal{T}$. A solution to overcome this problem is to replace the equality constraint (7) by the minimization problem

$$\text{minimize } \|\mathcal{T}\psi - z\|^2 \text{ subject to } \psi \in \mathcal{X}. \tag{8}$$

The set of solutions of (8) is denoted by $\text{argmin}_{\psi \in \mathcal{X}} \|\mathcal{T}\psi - z\|^2$. The following results can be found in [12, Chapter 4]:

- If \mathcal{T} is injective, then (8) has at most one solution.
- If $z \in \text{Im}\mathcal{T} \oplus (\text{Im}\mathcal{T})^\perp$, then the set $\text{argmin}_{\psi \in \mathcal{X}} \|\mathcal{T}\psi - z\|^2$ is closed, convex and non-empty (in particular (8) admits at least one solution).
- If \mathcal{T} is bijective and admits a left inverse denoted \mathcal{T}^{-1} then the unique solution of (8) is $\hat{\psi}(t) = \mathcal{T}^{-1}z(t)$.

For finite dimensional systems, the injectivity of \mathcal{T} is directly linked with an observability property of the dynamical system (1). Indeed, following [14], it can be shown that for finite dimensional systems, if the pair $(\mathcal{F}, \mathcal{H})$ is observable (in the sense that the Kalman observability matrix is full rank), then picking p pairwise distinct λ_i 's with $p = \dim \mathcal{X}$, then the obtained mapping \mathcal{T} is invertible. In that case, a KKL observer can simply be obtained as

$$\dot{z} = \begin{bmatrix} \lambda_1 & & \\ & \ddots & \\ & & \lambda_p \end{bmatrix} z + \begin{bmatrix} 1 \\ \vdots \\ 1 \end{bmatrix} y, \quad \hat{\psi}(t) = \mathcal{T}^{-1}z(t).$$

In the infinite dimensional case, there is no hope that a finite number of λ_i 's can give all the information allowing to reconstruct the entire system's state. It is an open question to know if observability properties of the infinite dimensional system allows to obtain that a certain countable set of λ_i 's gives enough information. In that case, the minimization problem (8) becomes ill-posed. In other words, it may have no solution, or numerous solutions, and its solutions may depend on z in a non-continuous manner. In our case, z is an estimation of $\mathcal{T}\psi$. Hence, the minimizer $\hat{\psi}$ of (8) may be very different of the real state ψ . A typical approach to overcome this problem is to consider a Tikhonov regularization method in which the optimization problem (8) is slightly modified. This new minimization problem will have solutions close to the former one, and be well-posed. We recall the next proposition on which this method is based for the convenience of the reader.

Proposition 2.2 ([12], Proposition 6.1). *Given \mathcal{T} in $\mathcal{L}(\mathcal{X}, \mathbb{R}^p)$ and $\delta > 0$, the minimization problem*

$$\text{minimize } \|\mathcal{T}\psi - z\|^2 + \delta\|\psi\|^2 \text{ subject to } \psi \in \mathcal{X} \quad (9)$$

admits a unique solution and is a continuous function of z in \mathbb{R}^p .

The choice of the *regularization parameter* δ is of the uttermost importance. Indeed, as $\delta \rightarrow +\infty$, the solution of (9) goes to zero. Conversely, as $\delta \rightarrow 0$, the problem (9) goes closer to the ill-posed problem (8). A compromise shall be made. In practice, δ is chosen experimentally, and is linked to the measure confidence: the more uncertain is the output y , the bigger is δ .

We also have the following theoretical result, that describes what happens when δ goes to zero.

Theorem 2.3 ([12, Theorem 6.1]). *Let \mathcal{T} in $\mathcal{L}(\mathcal{X}, \mathbb{R}^p)$ and $z \in \text{Im}\mathcal{T}$. Let $\psi_0 \in \mathcal{X}$ and ψ the solution of (8) closest to ψ_0 . Let $(z_n)_{n \in \mathbb{N}}$ be a sequence in \mathbb{R}^p converging to z . Let $\varepsilon_n = |z_n - z|$. Let $(\delta_n)_{n \in \mathbb{N}}$ be a sequence of regularization parameters converging to zero. For any $n \in \mathbb{N}$, let ψ_n be the solution of the problem (9) associated to z_n and δ_n . Then,*

- $|\mathcal{T}\psi_n - z_n| \xrightarrow{n \rightarrow +\infty} 0$;
- if $\frac{\varepsilon_n}{\delta_n} \xrightarrow{n \rightarrow +\infty} 0$, then $|\mathcal{T}\psi_n - z_n| = \mathcal{O}(\varepsilon_n)$ and $\psi_n \xrightarrow{n \rightarrow +\infty} \psi$;
- if $\frac{\varepsilon_n}{\delta_n^2} \xrightarrow{n \rightarrow +\infty} 0$ and $\psi \in (\text{Im}\mathcal{T})^*$, then $|\mathcal{T}\psi_n - z_n| = \mathcal{O}(\varepsilon_n^2)$ and $|\psi_n - \psi| = \mathcal{O}(\varepsilon_n)$.

To summarize, a possible observer design of a given abstract Cauchy problem in the form (1) is then given by

$$\begin{cases} \dot{z} = \begin{bmatrix} \lambda_1 & & \\ & \ddots & \\ & & \lambda_p \end{bmatrix} z + \begin{bmatrix} 1 \\ \vdots \\ 1 \end{bmatrix} y \\ \hat{\psi}(t) = \text{argmin}_{\psi \in \mathcal{X}} \{ \|\mathcal{T}\psi - z(t)\|^2 + \delta\|\psi\|^2 \}, \quad \delta > 0 \\ \mathcal{T} = (\mathcal{T}_{\lambda_1}, \dots, \mathcal{T}_{\lambda_p}), \quad \mathcal{T}_{\lambda_i} = \mathcal{H}(\mathcal{F} - \lambda_i I)^{-1}, \quad i = 1, \dots, p, \end{cases} \quad (10)$$

where the λ_i are pairwise distinct elements of $\rho(\mathcal{F}) \cap \mathbb{R}_-^*$.

Note that despite the fact that this dynamical system is well-defined for all abstract Cauchy problem in the form (1), its convergence to the real state is not guaranteed *a priori* and may be linked to observability properties.

3 Application to the crystallization process

3.1 Modeling the batch crystallization process

In this subsection, a dynamical model representing the batch crystallization process and the concentration measurement is given.

3.1.1 Population balance equation

In a first step a batch crystallization process is modeled. We assume that the size of the crystals is described by a scalar parameter x (in m). For example, if the crystals are spherical, then x may represent their diameter.

Let us denote $\psi(t, \cdot)$ the Number Density Function in terms of the crystal size (NDF) at time t (in $\text{m}^{-1}.\text{m}^{-3}$), so that $\int_{x_1}^{x_2} \psi(t, x) dx$ is the total amount of crystals in the reactor at time t with size between x_1 and x_2 (in m^{-3}). Let $[t_0, t_1]$ be the time window in which the crystallization process occurs.

We assume that the crystals never reach a specific maximal allowable size denoted x_{\max} during the experiment. Typically this size can simply be related to the size of the reactor in which the crystallization occurs:

$$\forall t \in [t_0, t_1], \quad \psi(t, x_{\max}) = 0. \quad (11)$$

We assume that all the crystals appear at the same positive size x_{\min} , and we denote $u(t)$ the appearance rate of new crystals at size x_{\min} at time t . The function u quantifies the nucleation rate in the reactor. In [22], for instance, an expression for the function u is given as $u(t) = R_n(t)/G(t)$, where R_n is the overall rate of nucleation expressed in $\text{s}^{-1}.\text{m}^{-3}$ and G is the growth rate of the crystals in $\text{m}.\text{s}^{-1}$. Note however that in our approach for NDF observation, we don't need to know precisely this expression. We do not use any model of u , and assume this quantity to be unknown. We have

$$\forall t \in [t_0, t_1], \quad \psi(t, x_{\min}) = u(t). \quad (12)$$

Finally, let $G(t, x) \geq 0$ be the growth rate of the crystals in $\text{m}.\text{s}^{-1}$, in other words the rate at which a crystal of size x grows at time t . The population balance leads to

$$\forall t \in (t_0, t_1), \quad \forall x \in (x_{\min}, x_{\max}), \quad \partial_t \psi(t, x) + \partial_x (G\psi)(t, x) = 0. \quad (13)$$

By considering the McCabe assumption, we assume that G does not depend on x . In that case equation (13) becomes

$$\forall t \in (t_0, t_1), \quad \forall x \in (x_{\min}, x_{\max}), \quad \partial_t \psi(t, x) + G(t) \partial_x \psi(t, x) = 0. \quad (14)$$

Equation (14) is a time-varying one-dimensional transport equation.

We also assume that at the beginning of the experiment, some seed particles are in the reactor. This yields

$$\forall x \in [x_{\min}, x_{\max}], \quad \psi(t_0, x) = \psi_0(x).$$

To summarize, the model of the NDF in a batch crystallization process is:

$$\begin{cases} \partial_t \psi(t, x) = -G(t) \partial_x \psi(t, x) & \forall t \in (t_0, t_1), \quad \forall x \in (x_{\min}, x_{\max}) \\ \psi(t_0, x) = \psi_0(x) & \forall x \in [x_{\min}, x_{\max}] \\ \psi(t, x_{\min}) = u(t) & \forall t \in [t_0, t_1] \end{cases} \quad (15)$$

to which is added the other boundary condition in (11) which in our case is seen as a knowledge on the particular solution we wish to estimate.

The following theorem states that system (15) of this model admits weak solution in L^2 space and strong solution in H^1 .

Theorem 3.1. Let $t_1 > t_0 \geq 0$, $x_{\max} > x_{\min} \geq 0$, $\psi_0 \in H^1(x_{\min}, x_{\max})$, $u \in H^1(t_0, t_1)$, $G \in C^0([t_0, t_1]; \mathbb{R}_+^*)$. Assume that $u(t_0) = \psi_0(x_{\min})$. Then system (15) admits a unique solution

$$\psi \in C^0([t_0, t_1]; H^1(x_{\min}, x_{\max})) \cap C^1([t_0, t_1]; L^2(x_{\min}, x_{\max})).$$

Moreover, for all $(t, x) \in [t_0, t_1] \times [x_{\min}, x_{\max}]$,

$$\psi(t, x) = \begin{cases} \psi_0(x - \mathfrak{G}(t)) & \text{if } x - x_{\min} \geq \mathfrak{G}(t) \\ u \circ \mathfrak{G}^{-1}(\mathfrak{G}(t) - x + x_{\min}) & \text{else.} \end{cases} \quad (16)$$

where $\mathfrak{G} : [t_0, t_1] \ni t \mapsto \int_{t_0}^t G(\tau) d\tau$.

The proof of this theorem can be found in [6, Theorem 2.4] in the case $G = 1$, and can be easily adapted by means of a time reparametrization. It is worth noticing that this theorem does not take into account hypothesis (11). However, the following proposition holds.

Proposition 3.2. Assume that the hypothesis of Theorem 3.1 are satisfied. Assume that there exists $\bar{x} \in [x_{\min}, x_{\max}]$ such that $\psi_0(x) = 0$ for all $x \in [\bar{x}, x_{\max}]$. If

$$\bar{x} + \mathfrak{G}(t_1) < x_{\max}, \quad (17)$$

then $\psi(t, x) = 0$ for all $t \in [t_0, t_1]$ and all $x \in [\bar{x} + \mathfrak{G}(t_1), x_{\max}]$.

Proof. Let $t \in [t_0, t_1]$ and $x \in [\bar{x} + \mathfrak{G}(t_1), x_{\max}]$. Then

$$x - \mathfrak{G}(t_1) \geq \bar{x} \geq x_{\min}.$$

Consequently, according to (16), $\psi(t, x) = \psi_0(x - \mathfrak{G}(t)) = 0$. □

Hence, one must choose t_1 small enough so that the particles did not reach the size x_{\max} . Roughly speaking, this means that the observer that we are going to design must estimate the state in small time, *i.e.* before the particles reach the size x_{\max} . In the following, we always assume that (11) is satisfied.

3.2 Concentration sensor modeling

In the considered batch crystallization process, the measured outputs are the temperature and the solute concentration denoted $C_c(t)$. These two measurements allow to obtain online estimation of the growth rate (*i.e.* G) and the third moment of the NDF.

3.2.1 Estimation of G

The knowledge of the temperature and the solute concentration allows to obtain some approximation of the growth rate G . Indeed, following [29], a model of G can be given for all time $t \in [t_0, t_1]$ by

$$G(t) = k_g \frac{C_c(t) - C^*(t)}{C^*(t)} \quad (18)$$

where

- k_g is a known growth rate parameter (in m.s^{-1}),
- $C^*(t)$ is the solubility at time t (in kg of solute per kg of solvent),
- $C_c(t)$ is the solute concentration at time t (in kg of solute per kg of solvent).

Since $C^*(t)$ depends on the temperature at time t , the growth rate G of the crystals can be estimated online with the available sensors.

Other model expressions of G are available in the literature, for more details one may refer to [16, 20].

3.2.2 Estimation of the third moment of the NDF

It is possible to link the solute concentration with the NDF. Indeed, for each $t \in \mathbb{R}_+$, let $C_s(t)$ (in kg of solid per kg of solvent) be the solid concentration in the reactor at time t , in other words, the ratio between the total crystals mass in the reactor at time t and the solvent mass. Let ρ_s (in kg.m^{-3}) be the density of the solute in solid phase and M_e the solvent mass (in kg). It yields:

$$C_s(t) = \frac{\rho_s}{M_e} V_s(t)$$

where $V_s(t)$ is the volume (in m^3) occupied by the crystals at time t . Then the volume of a crystal with size x (in m) is simply $V = k_v x^3$ where k_v is a volumetric shape factor (see *e.g.* [9, 26]). For example, $k_v = \pi/6$ for spherical crystals. The total volume of the crystals is then

$$V_s(t) = k_v \int_{x_{\min}}^{x_{\max}} \psi(t, x) x^3 dx$$

Hence, the solid concentration in the reactor can be expressed as follows.

$$\forall t \in [t_0, t_1], \quad C_s(t) = \frac{\rho_s k_v}{M_e} \int_{x_{\min}}^{x_{\max}} \psi(t, x) x^3 dx. \quad (19)$$

Assume moreover that ρ_s is a known parameter. This implies that we can associate to system (15) the measurement y defined as

$$\forall t \in [t_0, t_1], \quad y(t) = \int_{x_{\min}}^{x_{\max}} \psi(t, x) x^3 dx. \quad (20)$$

From there, the observation problem we intend to solve is the following. *From the knowledge of the output function $y(t)$ and the growth rate, give an online estimation of the NDF.*

The purpose of the Section 3.4 is to propose a novel algorithm to solve this problem based on the KKL methodology which was described in Section 2. Note however that before implementing the observer an observability analysis can be carried out.

3.3 About the observability of the crystallization model

In this section, we study how the third moment may help us to estimate the NDF. First, we have the following result.

Proposition 3.3. *Let $\tau \in (t_0, t_1]$. Assume that there exists $\mu > 0$ such that $G(t) \geq \mu$ for all $t \in [t_0, t_1]$. Then for all $y \in C^0(t_0, \tau)$, there exists at most one function $u \in H^4(t_0, \tau)$ such that the solution ψ of (15) given by u and $\psi_0 = 0$ satisfies*

$$y(t) = \int_{x_{\min}}^{x_{\max}} \psi(t, x) x^3 dx, \quad \forall t \in [t_0, \tau].$$

In other words, Proposition 3.3 states that the map $u \mapsto y$ is injective, where y denotes the third moment of the solution of (15) with null initial condition. Its proof can be found in appendix. Hence, one can hope that our method may reconstruct ψ from y , at least when the initial condition is zero (*i.e.* there is no crystals at the beginning of the process).

However, one can wonder what happens if the initial condition is not zero. Can we still reconstruct the state from the measurement of its third moment and the knowledge of its dynamics? In other words, is the map $\psi \mapsto y$ injective? If yes, then one can hope that our algorithm is robust, so that the estimation of the state converges to the actual NDF. Unfortunately, the answer is no. Indeed, we have the following proposition which is a slight modification of [30, Theorem 3.2.3] that we state in our own context only. For the convenience of the reader, its proof is given in appendix.

Proposition 3.4. *Let $\tau \in (t_0, t_1]$. Assume that there exists $\mu > 0$ such that $G(t) \geq \mu$ for all $t \in [t_0, t_1]$. There exist infinitely many solutions of (15) with different initial conditions and boundary conditions that have the same third moment $y \in C^0(t_0, \tau)$.*

We shall say that system (15) with measurement (20) is not observable. Thus, we cannot guarantee that our estimation of the NDF converges to the actual NDF. Despite this fact, our methodology should be able to reconstruct partially the actual NDF. Indeed, the linear function that maps the NDF to its third moment has rank 4. The image of this state-output mapping is sometimes called the *observable part* of the system (see *e.g.* [8]), due to the fact that an observer shall estimate at least the projection of the actual state on this subspace. See the proof in appendix for more details.

3.4 A dynamical observer from the concentration measurement

Eventhough it was shown in the former section that the system is not observable, in this subsection, we show how the KKL observer approach can be employed on the considered model. Following the procedure given in Section 2, we consider λ a negative real number and the dynamical system

$$\dot{z} = \lambda z + y. \quad (21)$$

We must find a mapping \mathcal{T}_λ which is estimated by this dynamical equation. We have the following proposition.

Proposition 3.5. *Let $\mathcal{T}_\lambda : C^1([t_0, t_1]; L^2(x_{\min}, x_{\max})) \mapsto C^1([t_0, t_1])$ be the functional defined as*

$$\mathcal{T}_\lambda(\psi) : t \mapsto \int_{x_{\min}}^{x_{\max}} a(t, x) \psi(t, x) dx \quad (22)$$

where

$$\begin{cases} \partial_t a(t, x) + G(t)\partial_x a(t, x) = \lambda a(t, x) + x^3 & \forall t \in (t_0, t_1), \forall x \in (x_{\min}, x_{\max}) \\ a(t_0, x) = 0 & \forall x \in [x_{\min}, x_{\max}] \\ a(t, x_{\min}) = 0 & \forall t \in [t_0, t_1], \end{cases} \quad (23)$$

then, along the solution of (21) which satisfies (11) where y is given in (20), it yields for all t in $[t_0, t_1]$

$$\mathcal{T}_\lambda(\psi)(t) - z(t) = \exp(\lambda t)(\mathcal{T}_\lambda(\psi)(0) - z_0). \quad (24)$$

Proof. Using (15) and an integration by parts yields

$$\begin{aligned} \frac{d}{dt}(\mathcal{T}_\lambda(\psi)(t) - z(t)) &= \int_{x_{\min}}^{x_{\max}} \partial_t a(t, x)\psi(t, x)dx - \int_{x_{\min}}^{x_{\max}} G(t)a(t, x)\partial_x \psi(t, x)dx \\ &\quad - \lambda z(t) - \int_{x_{\min}}^{x_{\max}} x^3 \psi(t, x)dx \\ &= \int_{x_{\min}}^{x_{\max}} \partial_t a(t, x)\psi(t, x)dx + \int_{x_{\min}}^{x_{\max}} G(t)\partial_x a(t, x)\psi(t, x)dx \\ &\quad - G(t)[a(t, x)\psi(t, x)]_{x_{\min}}^{x_{\max}} - \lambda z(t) - \int_{x_{\min}}^{x_{\max}} x^3 \psi(t, x)dx. \end{aligned}$$

Hence, with (23) and also the boundary condition in (15) and (11), this implies

$$\frac{d}{dt}(\mathcal{T}_\lambda(\psi)(t) - z(t)) = \lambda(\mathcal{T}_\lambda(\psi)(t) - z(t)).$$

By integrating in time the former equation, we obtain (24). \square

Consequently, for each negative λ we exponentially estimate the functional $\mathcal{T}_\lambda \psi(t)$. It is interesting to remark that no information on the nucleation rate is needed to obtain this estimation. The state observer is given as (10), after a choice of the regularization parameter δ .

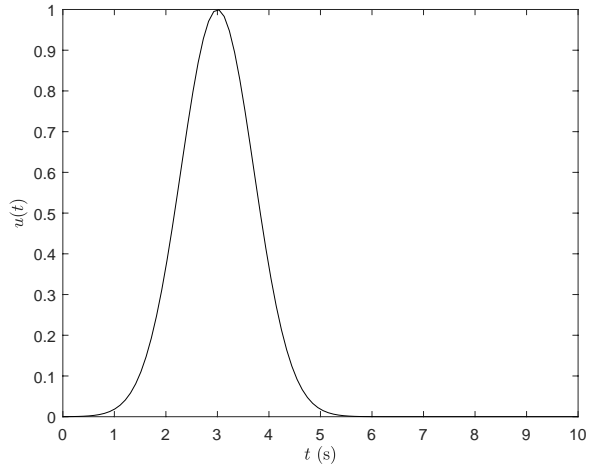
4 Numerical simulations

In this subsection numerical simulations are carried out. Let $(x_j)_{1 \leq j \leq N_x}$ be a uniform discretization of the space interval (x_{\min}, x_{\max}) with space step Δx and $(t_k)_{1 \leq k \leq N_t}$ be a uniform discretization of the time interval (t_0, t_1) with time step Δt . We fix $N_x = N_t = 100$. Let $(\lambda_j)_{1 \leq j \leq p}$ be the considered negative values of λ . An approximation of $(\mathcal{T}_{\lambda_i} \psi)(t_k)$ is given by $\Delta x \sum_{j=1}^{N_x} a_{i,j,k} \psi_{j,k}$ where $a_{i,j,k}$ is an approximation of $a_{\lambda_i}(t_k, x_j)$ (solution of (23)) and $\psi_{j,k}$ an approximation of $\psi(t_k, x_j)$. The transport equation which describes the crystallization process is simulated via the method of characteristics.

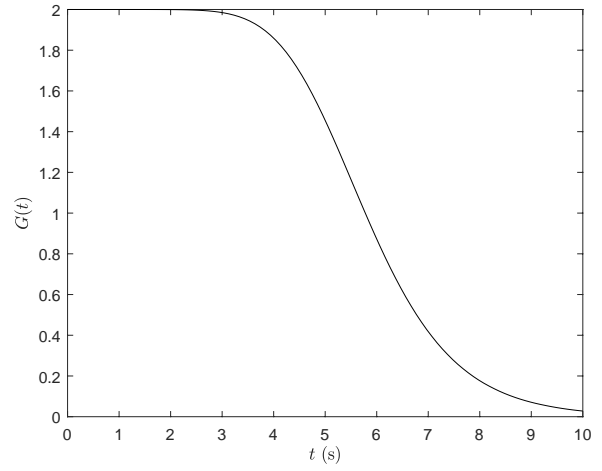
We consider the system (15) with G as in (18) with a null initial condition $\psi_0 = 0$ and a boundary condition similar to a truncated normal distribution reaching its maximum at $t = 3$ s and with a compact support $[0, 6]$ (see Fig. 1a). The unique solution of this system is drawn in Fig. 1c (solid line), and the corresponding growth rate is drawn in Fig. 1b.

4.1 Step 1: reconstruction of a function of the state

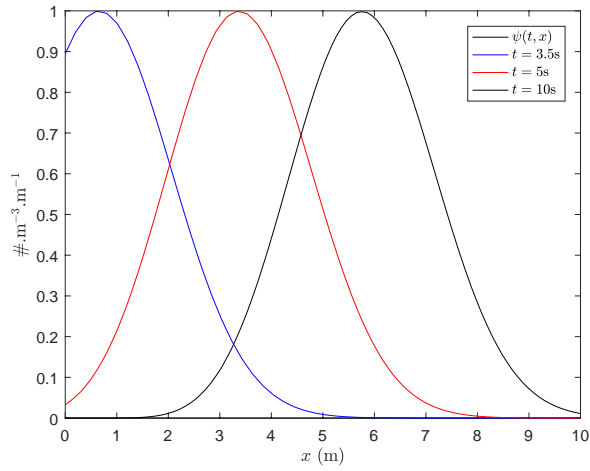
Following the methodology developed in Section 2, we first try to estimate the function $\mathcal{T}_\lambda(\psi)$ of the state via the dynamical system (21) for some fixed negative values of λ . All along the simulation of (15), we compute y and



(a) Boundary condition u due to the nucleation



(b) Growth rate G , given by (18)



(c) Simulation of the NDF ψ

Figure 1: Numerical simulation of the process with $(x_{\min}, x_{\max}) = (0, 10)$, $(t_0, t_1) = (0, 10)$ and $N_x = N_t = 100$.

estimate the solution of (23) via the method of characteristics. We integrate the solution of (21) with the first order Euler's method. Then we plot the evolution of the relative error between z and $\mathcal{T}_\lambda(\psi)$ in Fig. 2 for some values of λ . One can check that the error goes to zero as $t \rightarrow +\infty$. Moreover, the bigger is $|\lambda|$, the faster is the convergence. This is due to the exponential convergence of $z - \mathcal{T}_\lambda(\psi)$ to zero given by (4). Hence, we are able to approximate any function $\mathcal{T}_\lambda(\psi)$ of the state. Now, we can move to the second part of the methodology of Section 2.

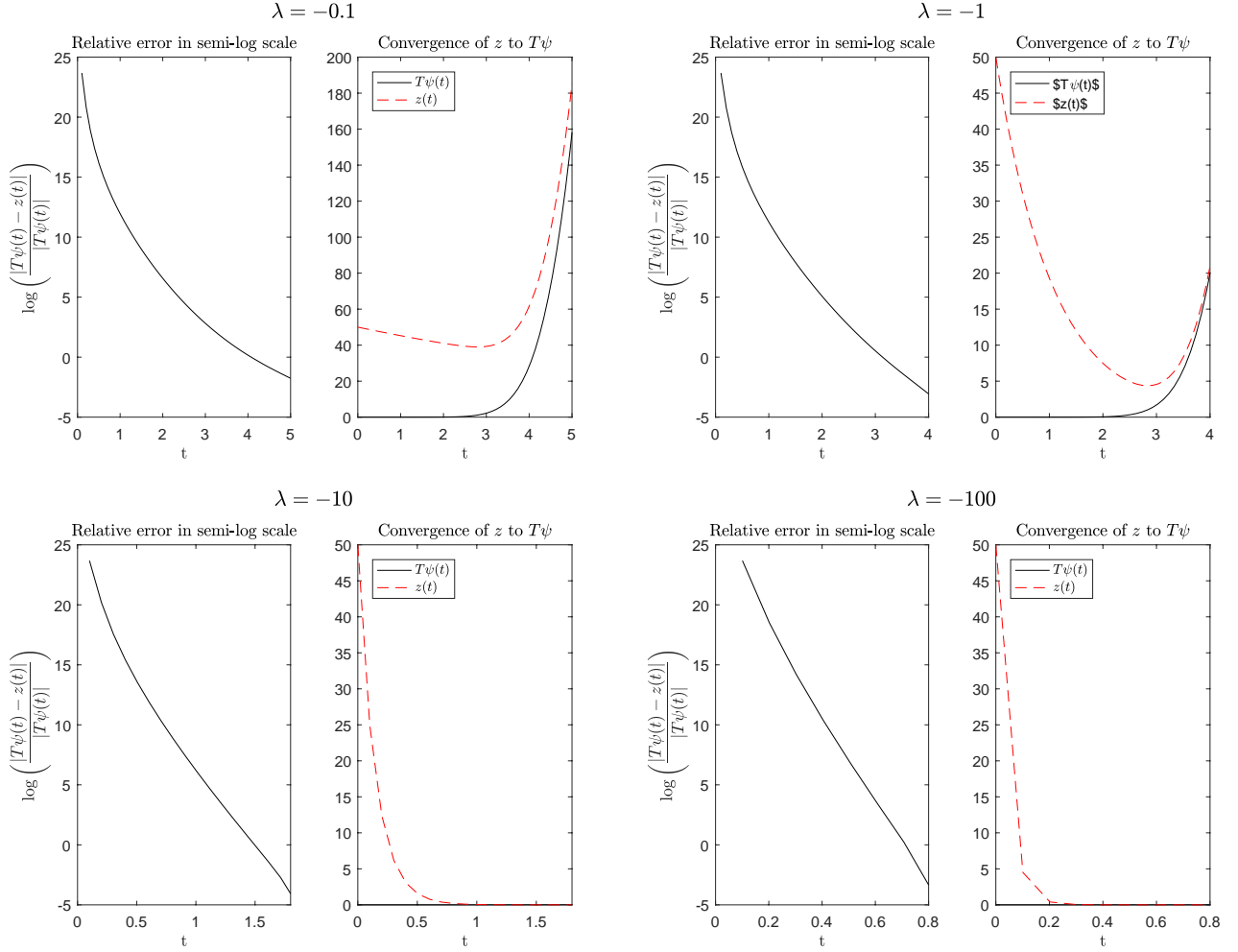


Figure 2: Convergence of $\mathcal{T}_\lambda(\psi) - z$ to zero for different values of λ . We choose $z(0) \neq 0$ arbitrarily. The bigger is $|\lambda|$, the faster is the convergence. By means of a linear regression, one can estimate the convergence rate of the relative error to zero: $\mathcal{O}(e^{-7.4t})$ if $\lambda = -0, 1$, $\mathcal{O}(e^{-8.2t})$ if $\lambda = -1$, $\mathcal{O}(e^{-14.2t})$ if $\lambda = -10$, $\mathcal{O}(e^{-32.9t})$ if $\lambda = -100$.

4.2 Step 2: reconstruction of the entire state of the system

Following Step 1, we estimate simultaneously numerous functions $\mathcal{T}_{\lambda_i}(\psi)$ which correspond to different values $\lambda_i < 0$. These estimations are denoted z_{λ_i} . The aim of this section is to estimate the state ψ from the knowledge of $(z_{\lambda_i})_{1 \leq i \leq p}$.

Then, we choose a regularization parameter $\delta > 0$ and solve the discrete version of the quadratic minimization

problem (9) at each time step, that is for each time \mathbb{k} , find $(\psi_{j,k})_{1 \leq j \leq N_x}$ that

$$\text{minimize } \left\| \Delta x (a_{i,j,k})_{1 \leq i \leq p, 1 \leq j \leq N_x} \cdot (\psi_{j,k})_{1 \leq j \leq N_x} - (z_{\lambda_i}(\mathbb{k}_k))_{1 \leq i \leq p} \right\|^2 + \delta \left\| (\psi_{j,k})_{1 \leq j \leq N_x} \right\|^2. \quad (25)$$

This is a quadratic minimization problem, which we solve via an interior-point method (see *e.g.* [5, Chapter III.11]). We need to fix an initial condition to apply this algorithm. Following a continuation method, we choose as an initial condition at time \mathbb{k} the minimum value obtained at time \mathbb{k}_{k-1} , transported during a time Δt at speed $G(\mathbb{k}_{k-1})$.

The choice of parameters p , $\lambda_1, \dots, \lambda_p$ and δ and their influence are investigated in the paragraphs below.

- **Choice of the p and (λ_i) .** Note that the matrix $(a_{i,j,k})_{1 \leq i \leq p, 1 \leq j \leq N_x}$ may be injective only if $p \geq N_x$, that is if the discretization in λ is thinner than in x . Therefore, we fix $p = 2N_x = 200$. Moreover, even if the matrix $(a_{i,j,k})_{i,j}$ is injective, a regularization method is needed to left-inverse it. Indeed, for all $t \in (t_0, t_1)$, the operator

$$L^2(x_{\min}, x_{\max}) \ni \psi \mapsto \left(\lambda \mapsto \int_{x_{\min}}^{x_{\max}} a_\lambda(t, x) \psi(x) dx \right) \in L^2(\lambda_{\min}, \lambda_{\max})$$

is compact (as an integral operator). Hence, even if it is injective, its inverse is not continuous. The matrix $(a_{i,j,k})_{i,j}$ is a discretization of this operator. Then, the more the discretization is thinner, the more it is ill-conditioned. This emphasizes the necessity of using a regularization method.

In Fig. 3, we plot the estimation of the NDF for different values of (λ_i) . For large values of $|\lambda|$, z converges quickly to $\mathcal{T}\psi$. However, it appears that functions a_λ carry less information for large values of $|\lambda|$, so that the map \mathcal{T} is more difficult to inverse. This explains Fig. 3b, on which the estimation $\hat{\psi}$ is worst than on Fig. 3c.

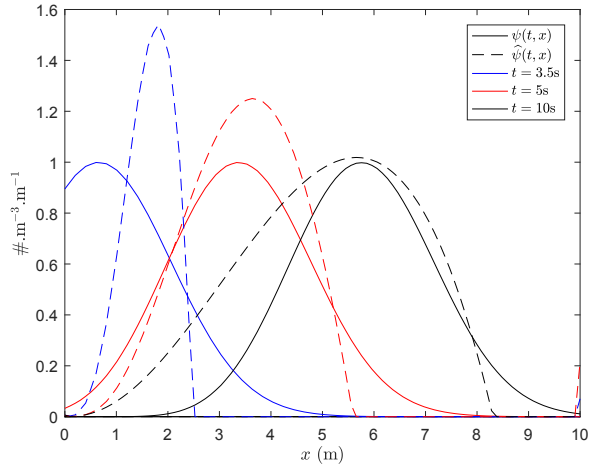
On the contrary, for small values of $|\lambda|$, it seems that functions a_λ carry more information, since the estimation $\hat{\psi}$ is similar on Fig. 3a and Fig. 3c at $t = 10$ s. However, we also see a peaking phenomenon (for $t \leq 5$ s on Fig. 3a), due to the fact that z is slower to converge to $\mathcal{T}\psi$ than for large values of $|\lambda|$.

Thus, one must find a compromise for the choice of (λ_i) : take large values for fast convergence and avoiding peaking, and small values for efficient estimation.

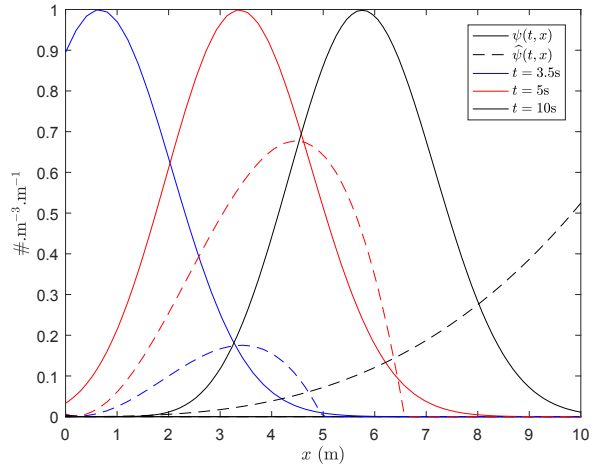
- **Choice of the regularization parameter δ .**

The regularization parameter δ must be chosen numerically, in order to find a compromise between the minimization of the norm of the state, and the minimization of the gap $\mathcal{T}\psi - z$. This compromise can be interpreted as a measurement reliability. Indeed, if the measurement has a small uncertainty, then we choose a small δ . On the contrary, if the measurement is highly uncertain, then we fix a large value of δ in order to regularize the solution.

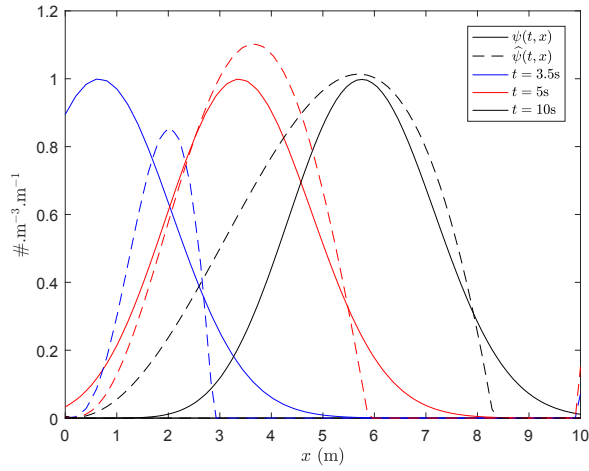
In Fig. 4, we plot the actual NDF ψ and its estimation $\hat{\psi}$ at different times, for different values of δ , and with or without measurement noise. Measurement noise is fixed at 2% of the maximal value of the output on the time interval. For small values of δ and/or with measurement noise, we see that a peaking phenomenon appear: this is due to a lack of regularization of the solution. On the contrary, if δ is too large, then the minimization of the norm of the state takes too much importance in the minimization problem, and $\hat{\psi}$ is too attenuated.



(a) $(\lambda_i) \subset [-10, -1]$

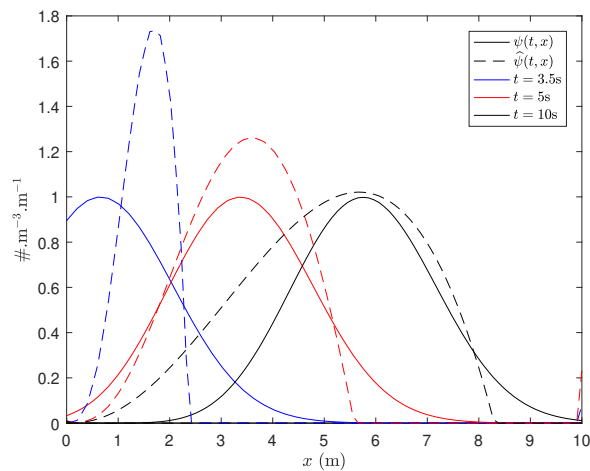


(b) $(\lambda_i) \subset [-100, -10]$

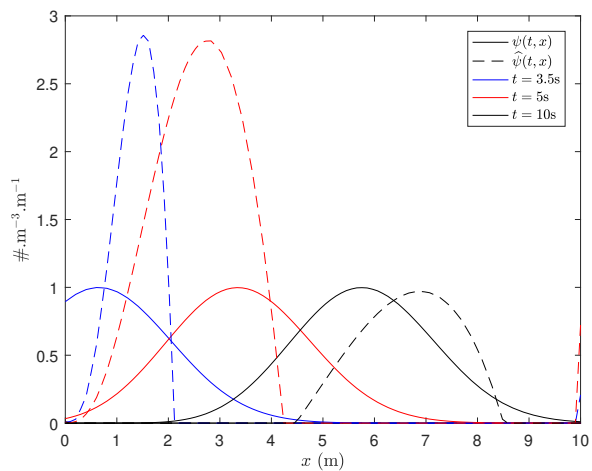


(c) $(\lambda_i) \subset [-100, -1]$

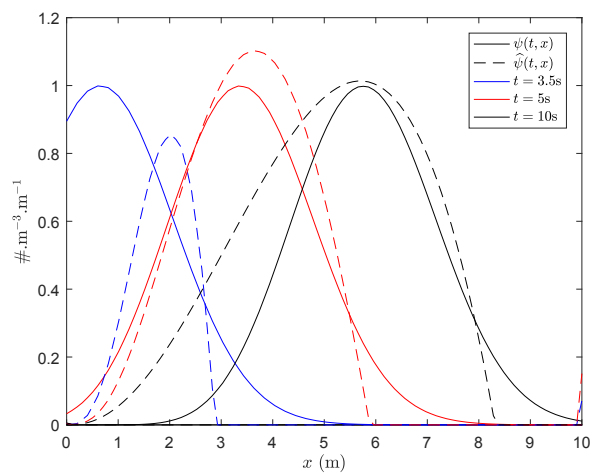
Figure 3: Influence of $(\lambda_i)_{1 \leq i \leq p}$ on the reconstruction of the CSD.



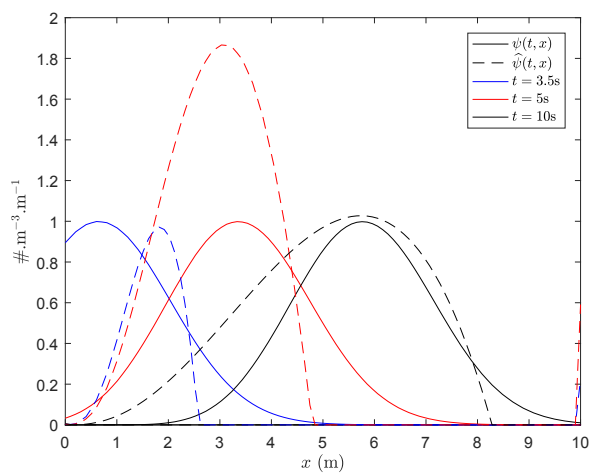
(a) $\delta = 0.05, \alpha = 0$



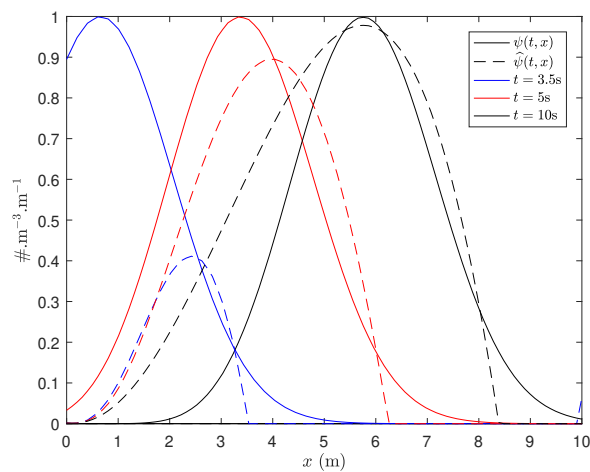
(b) $\delta = 0.05, \alpha = 2\%$



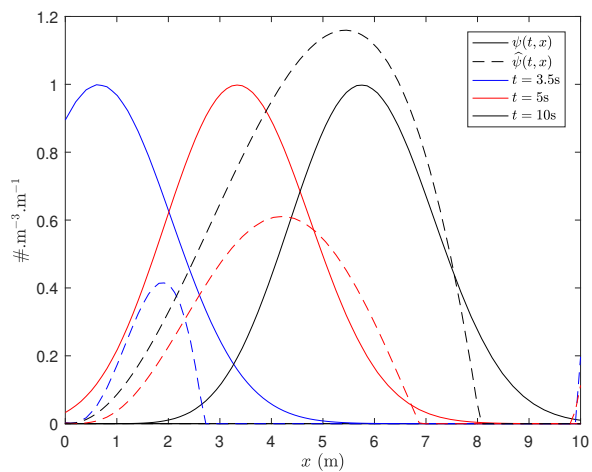
(c) $\delta = 0.1, \alpha = 0$



(d) $\delta = 0.1, \alpha = 2\%$



(e) $\delta = 0.2, \alpha = 0$



(f) $\delta = 0.2, \alpha = 2\%$

Figure 4: Influence of the regularization parameter δ and measurement noise α on the reconstruction of the CSD

5 Conclusion

In this paper a new observer has been introduced to estimate the Crystal Size Distribution from the measurements of the solute concentration, temperature and a model of the growth rate. No model of the nucleation rate is needed. This approach is based on the use of Kazantzis-Kravaris/Luenberger observer and a Tikhonov regularization procedure. The numerical results obtained are promising. Even though, the knowledge of the solute concentration alone does not allow to accurately reconstruct the full CSD as shown by our observability analysis, we believe that this tool could be used in addition with supplementary information given by other sensors (for instance FBRM[®]). This approach will be evaluated on experiments in a future research project.

Appendix: proofs of Propositions 3.3 and 3.4.

Assume that $G \geq \mu > 0$. Let $\tau \in (t_0, t_1]$ and $u \in H^4(t_0, \tau)$. Let ψ be the solution of (15) with initial condition ψ_0 and boundary condition u . We introduce a time reparametrization $\tilde{t} = \int_{t_0}^t G(s)ds$, which is well defined since $G \geq \mu$. Let $\tilde{\psi}$, \tilde{u} and \tilde{y} be such that $\tilde{\psi}(\tilde{t}) = \psi(t)$, $\tilde{u}(\tilde{t}) = u(t)$ and $\tilde{y}(\tilde{t}) = y(t)$ for all $t \in [t_0, t_1]$. Then

$$\begin{cases} \partial_{\tilde{t}} \tilde{\psi}(\tilde{t}, x) = -\partial_x \tilde{\psi}(\tilde{t}, x) \\ \tilde{\psi}(t_0, x) = \psi_0(x) \\ \tilde{\psi}(\tilde{t}, x_{\min}) = \tilde{u}(\tilde{t}) \end{cases} \quad (26)$$

and $\tilde{y}(\tilde{t}) = \int_{x_{\min}}^{x_{\max}} \tilde{\psi}(\tilde{t}, x)x^3 dx$. Since the observability properties are not affected by the time reparametrization, one can investigate observability properties of the system (26) instead of (15). Therefore, one can assume without loss of generality that $G = 1$ in the rest of the proof. Since $u \in H^4(t_0, \tau)$, we have $y \in C^4(t_0, \tau)$. Equation (11) and system (15) yield

$$\begin{aligned} y' &= 3 \int_{x_{\min}}^{x_{\max}} x^2 \psi(\cdot, x) dx - [x^3 \psi(\cdot, x)]_{x_{\min}}^{x_{\max}} \\ &= 3 \int_{x_{\min}}^{x_{\max}} x^2 \psi(\cdot, x) dx + x_{\min}^3 u, \end{aligned} \quad (27)$$

$$\begin{aligned} y^{(2)} &= 6 \int_{x_{\min}}^{x_{\max}} x \psi(\cdot, x) dx + 3 [x^2 \psi(\cdot, x)]_{x_{\min}}^{x_{\max}} + x_{\min}^3 u' \\ &= 6 \int_{x_{\min}}^{x_{\max}} x \psi(\cdot, x) dx + 3x_{\min}^2 u + x_{\min}^3 u', \end{aligned} \quad (28)$$

$$\begin{aligned} y^{(3)} &= 6 \int_{x_{\min}}^{x_{\max}} \psi(\cdot, x) dx - 6 [x \psi(\cdot, x)]_{x_{\min}}^{x_{\max}} + 3 x_{\min}^2 u' + x_{\min}^3 u^{(2)} \\ &= 6 \int_{x_{\min}}^{x_{\max}} \psi(\cdot, x) dx + 6x_{\min} u + 3x_{\min}^2 u' + x_{\min}^3 u^{(2)}, \end{aligned} \quad (29)$$

$$\begin{aligned} y^{(4)} &= -6 [\psi(\cdot, x)]_{x_{\min}}^{x_{\max}} + 6x_{\min} u' + 3x_{\min}^2 u^{(2)}(t) + x_{\min}^3 u^{(3)} \\ &= 6u + 6x_{\min} u' + 3x_{\min}^2 u^{(2)} + x_{\min}^3 u^{(3)}. \end{aligned} \quad (30)$$

End of the proof of Proposition 3.3. By hypothesis, $\psi_0 = 0$. Consequently, Equations (27)–(29) yield

$$\begin{cases} y'(t_0) = x_{\min}^3 u(t_0) \\ y^{(2)}(t_0) = 3x_{\min}^2 u(t_0) + x_{\min}^3 u'(t_0) \\ y^{(3)}(t_0) = 6x_{\min} u(t_0) + 3x_{\min}^2 u'(t_0) + x_{\min}^3 u^{(2)}(t_0), \end{cases}$$

which is a triangular system with non vanishing diagonal since $x_{\min} > 0$. Hence $u(t_0)$, $u'(t_0)$ and $u^{(2)}(t_0)$ are determined by y . Moreover, on $[t_0, \tau]$, u satisfies Equation (30) which is a 3rd order ordinary differential equation. Hence, according to the Cauchy-Lipschitz theorem, there exists a unique solution u to this problem. Thus y determines u uniquely, that $u \mapsto y$ is injective. \square

End of the proof of Proposition 3.4. Substituting the boundary condition in equation (30) with $u = 0$ yields $y^{(4)} = 0$ identically on $[t_0, \tau]$. Hence y is a polynomial function of degree less or equal than 3. Thus the linear function that maps any solution of (15) with null boundary condition to its third moment has rank 4. Since ψ lies in an infinite dimensional vector space, we get by the rank-nullity theorem that its kernel is non-trivial, *i.e.* the state-output map $\psi \mapsto y$ is not injective, and the system has a 4-dimensional observable part. \square

Note that Proposition 3.4 relies deeply on Hypothesis (11). Hence the non-injectivity of the measurement is due to the fact that the system is observed on a too small time interval. If the system was observed on $[t_0, +\infty)$, then one could show with similar arguments an injectivity result.

References

- [1] V. Andrieu and L. Praly. On the existence of a kazantzis–kravaris/luenberger observer. *SIAM Journal on Control and Optimization*, 45:432–456, 02 2006.
- [2] P. Bernard. *Observer Design for Nonlinear Systems*, volume 479 of *Lecture Notes in Control and Information Sciences*. Springer International Publishing, 2019.
- [3] P. Bernard and V. Andrieu. Luenberger observers for nonautonomous nonlinear systems. *IEEE Transactions on Automatic Control*, 69:270–281, 2019.
- [4] B. Biscans. Cristallisation en solution - Procédés et types d'appareils. *Techniques de l'ingénieur. Génie des procédés*, J2788 v2:1–25, 2013.
- [5] S. Boyd and L. Vandenberghe. *Convex Optimization*. Cambridge University Press, New York, NY, USA, 2004.
- [6] J. Coron. *Control and Nonlinearity*. Mathematical surveys and monographs. American Mathematical Society, 2007.
- [7] C. A. Dorao and H. A. Jakobsen. Numerical calculation of the moments of the population balance equation. *Journal of Computational and Applied Mathematics*, 196:619–633, 2006.
- [8] G. Haine. Recovering the observable part of the initial data of an infinite-dimensional linear system with skew-adjoint generator. *Mathematics of Control, Signals, and Systems*, 26(3):435–462, 2014.
- [9] H. Hulburt and S. Katz. Some problems in particle technology: A statistical mechanical formulation. *Chemical Engineering Science*, 19(8):555–574, 1964.

- [10] V. John, I. Angelov, A. A. Öncül, and D. Thévenin. Techniques for the reconstruction of a distribution from a finite number of its moments. *Chemical Engineering Science*, 62:2890–2904, 2007.
- [11] N. Kazantzis and C. Kravaris. Nonlinear observer design using lyapunov’s auxiliary theorem. *Systems & Control Letters*, 34(5):241–247, 1998.
- [12] M. Kern. *Méthodes numériques pour les problèmes inverses*. Mathématiques et statistiques. ISTE editions, 2016.
- [13] N. Lebaz, A. Cockx, M. Spérandio, and J. Morchain. Reconstruction of a distribution from a finite number and its moments : A comparative study in the case of depolymerization process. *Computers & Chemical Engineering*, 84:326–337, 2016.
- [14] D. G. Luenberger. Observing the state of a linear system. *IEEE Transactions on Military Electronics*, 8(2):74–80, April 1964.
- [15] D. G. Luenberger. An introduction to observers. *IEEE Transactions on automatic control*, 16(6):596–602, 1971.
- [16] A. Mersmann, A. Eble, and C. Heyer. Crystal growth. In A. Mersmann, editor, *Crystallization Technology Handbook*, pages 48–111. Marcel Dekker Inc., 2001.
- [17] A. Mesbah, A. E. Huesman, H. J. Kramer, Z. K. Nagy, and P. M. Van den Hof. Real-time control of a semi-industrial fed-batch evaporative crystallizer using different direct optimization strategies. *AIChE journal*, 57(6):1557–1569, 2011.
- [18] A. Mesbah, A. E. Huesman, H. J. Kramer, and P. M. Van den Hof. A comparison of nonlinear observers for output feedback model-based control of seeded batch crystallization processes. *Journal of Process Control*, 21(4):652–666, 2011.
- [19] S. Motz, S. Mannal, and E. D. Gilles. State estimation in batch crystallization using reduced population models. *Journal of Process Control*, 18(3-4):361–374, 2008.
- [20] J. Mullin. *Crystallization*. Elsevier, 4 edition, 2001.
- [21] Z. K. Nagy and R. D. Braatz. Robust nonlinear model predictive control of batch processes. *AIChE Journal*, 49(7):1776–1786, 7 2003.
- [22] Z. K. Nagy, G. Fevotte, H. Kramer, and L. L. Simon. Recent advances in the monitoring, modelling and control of crystallization systems. *Chemical Engineering Research and Design*, 91(10):1903–1922, 2013.
- [23] H. M. Omar and S. Rohani. Crystal Population Balance Formulation and Solution Methods : A Review. *Crystal Growth & Design*, 17:4028–4041, 2017.

- [24] I. B. Poblete, C. A. Castor, M. Nele, and J. C. Pinto. On-line monitoring of chord distributions in liquid–liquid dispersions and suspension polymerizations by using the focused beam reflectance measurement technique. *Polymer Engineering and Science*, 56:309–318, 2016.
- [25] M. Porru and L. Özkan. Monitoring of batch industrial crystallization with growth, nucleation, and agglomeration. part 2: Structure design for state estimation with secondary measurements. *Industrial & engineering chemistry research*, 56(34):9578–9592, 2017.
- [26] A. D. Randolph and M. A. Larson. *Theory of particulate processes*. Academic Press, 2 edition, 1988.
- [27] S. Scheler. Ray tracing as a supportive tool for interpretation of fbrm signals from spherical particles. *Chemical Engineering Science*, 101:503–514, 2013.
- [28] M. Tucsnak and G. Weiss. *Observation and Control for Operator Semigroups*. Birkhäuser Advanced Texts Basler Lehrbücher. Birkhäuser Basel, 2009.
- [29] B. Ucheddu, K. Zhang, H. Hammouri, and G. Févotte. Design of a csd observer during batch cooling crystallization dealing with uncertain nucleation parameters. *IFAC Proceedings Volumes*, 44(1):10460–10465, 2011.
- [30] J. A. W. Vissers. *Model-based estimation and control methods for batch cooling crystallizers*. PhD thesis, Technische Universiteit Eindhoven, 2012.